

# Evaluating the Potential of Ozone Microbubbles for Inactivation of Tulane Virus, a Human Norovirus Surrogate

Bozhong Guan, Haknyeong Hong, Minji Kim, Jiakai Lu,\* and Matthew D. Moore\*

Cite This: *ACS Omega* 2024, 9, 23184–23192

Read Online

ACCESS |



Metrics &amp; More

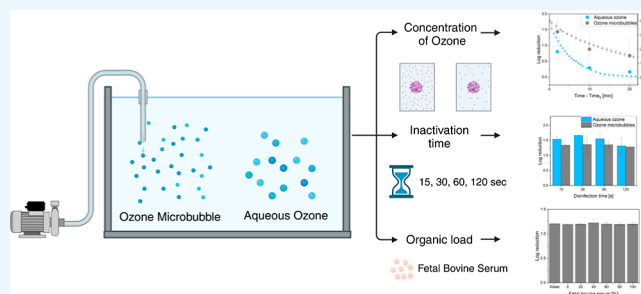


Article Recommendations



Supporting Information

**ABSTRACT:** This study investigated the efficacy of low-dose ozone microbubble solution and conventional aqueous ozone as inactivation agents against Tulane virus samples in water over a short period of time. Noroviruses are the primary cause of foodborne illnesses in the US, and the development of effective inactivation agents is crucial. Ozone has a high oxidizing ability and naturally decomposes to oxygen, but it has limitations due to its low dissolution rate, solubility, and stability. Ozone microbubbles have been promising in enhancing inactivation, but little research has been done on their efficacy against noroviruses. The study examined the influence of the dissolved ozone concentration, inactivation duration, and presence of organic matter during inactivation. The results showed that ozone microbubbles had a longer half-life ( $14 \pm 0.81$  min) than aqueous ozone ( $3 \pm 0.35$  min). After 2, 10, and 20 min postgeneration, the ozone concentration of microbubbles naturally decreased from 4 ppm to  $3.2 \pm 0.2$ ,  $2.26 \pm 0.19$ , and  $1.49 \pm 0.23$  ppm and resulted in  $1.43 \pm 0.44$ ,  $0.88 \pm 0.5$ , and  $0.68 \pm 0.53$   $\log_{10}$  viral reductions, respectively, while the ozone concentration of aqueous ozone decreased from 4 ppm to  $2.52 \pm 0.07$ ,  $0.43 \pm 0.05$ , and  $0.09 \pm 0.01$  ppm and produced  $0.8 \pm 0.28$ ,  $0.29 \pm 0.41$ , and  $0.16 \pm 0.21$   $\log_{10}$  reductions against Tulane virus, respectively ( $p = 0.0526$ ), suggesting that structuring of ozone in the bubbles over the applied treatment conditions did not have a significant effect, though future study with continuous generation of ozone microbubbles is needed.



## 1. INTRODUCTION

Human norovirus is the leading cause of foodborne illnesses in the United States and globally.<sup>1,2</sup> Noroviruses have several properties that make them difficult to control, including a low infectious dose,<sup>3</sup> high viral load shed by infected individuals,<sup>4</sup> and the ability to persist in foods and the environment for weeks to months.<sup>5,6</sup> Further, one of the major hurdles to controlling human noroviruses is the lack of efficacy of the active ingredients of many commonly used disinfectants, especially those approved for direct application on foods.<sup>7,8</sup> Sodium hypochlorite has been shown to be efficacious against noroviruses and other nonenveloped viruses at relatively high concentrations,<sup>9,10</sup> but chlorine exhibits instability when introduced to water, leading to reactions with both organic and inorganic substances. These interactions can give rise to byproducts that pose potential risks to human health and the environment,<sup>11</sup> which can damage organs, leading to cancer and other diseases.<sup>12,13</sup> Other commonly utilized disinfectants like alcohol,<sup>14</sup> UV light,<sup>15</sup> and quaternary ammonium compounds<sup>16</sup> have limitations as to whether they are able to be applied to foods or food contact surfaces and also may have harmful health and environmental effects. A good deal of research has been focused on plant-derived extracts and essential oils, with mixed results for efficacy against noroviruses;<sup>17</sup> however, many of these products also suffer from cost constraints and a lack of scalability for application to

larger aqueous systems like produce washes and depuration water treatment.

Due to the historical lack of *in vitro* human norovirus cultivation assays, as well as inherent limitations in existing human norovirus infectivity models,<sup>18</sup> many norovirus inactivation studies commonly rely on genetically and structurally related cultivable surrogate viruses.<sup>19,20</sup> Tulane virus is a norovirus surrogate that replicates in the intestinal tracts of rhesus macaques and has similar properties to human noroviruses, being a member of the *Caliciviridae* family, with single-stranded RNA and a nonenveloped T = 3 icosahedral capsid.<sup>21</sup> Compared to other human norovirus surrogates, Tulane virus has the advantage of being able to recognize the same putative cofactor as human noroviruses, while other surrogates do not.<sup>22,23</sup>

Ozone is a strong oxidant with high permeability that naturally breaks down to oxygen and does not form carcinogenic byproducts like chlorine.<sup>24</sup> Numerous reports

Received: October 24, 2023

Revised: May 11, 2024

Accepted: May 15, 2024

Published: May 22, 2024



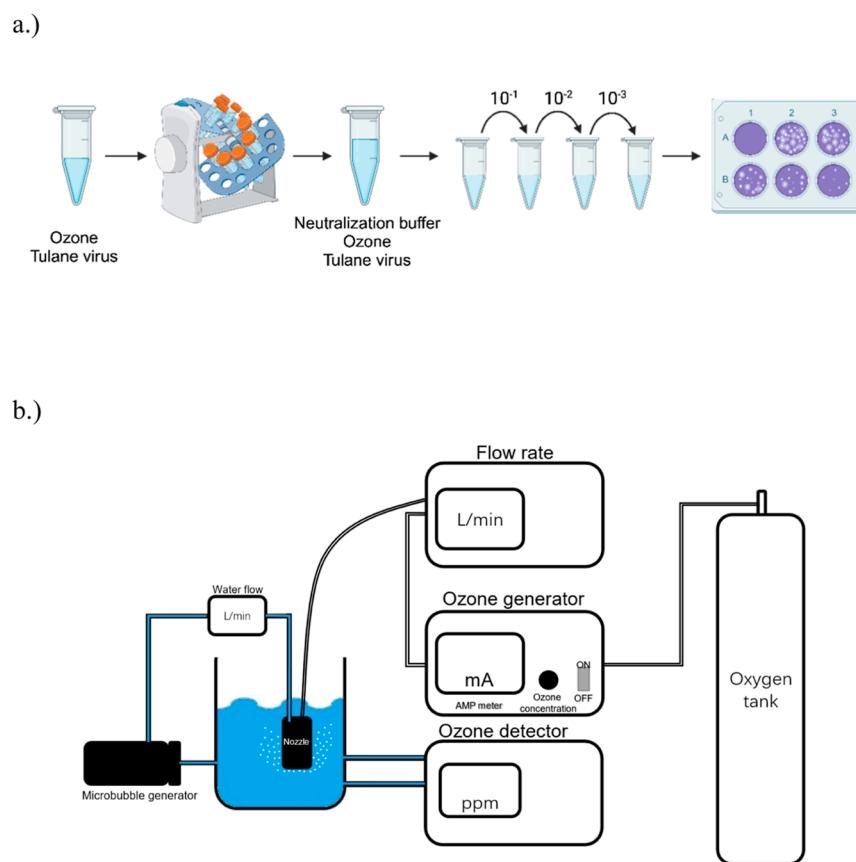


**Figure 1.** Schematic of experimental design of (a) inactivation treatment with suspension assay created with BioRender.com. Different concentrations of aqueous ozone or ozone microbubbles (0–4 ppm) that were pregenerated were mixed with Tulane virus for different time periods (0–20 min) and inactivation measured via the plaque assay. (b) Ozone microbubble generation setup.

have demonstrated that ozone shows favorable inactivation efficacy on bacterial pathogens,<sup>25</sup> fungi,<sup>26</sup> and spores.<sup>27</sup> Additionally, ozone has been shown to prevent viral attachment to host receptors by disruption of viral capsid or surface protein,<sup>28,29</sup> and it has shown some promise for the inactivation of several human norovirus surrogates, such as murine norovirus, feline calicivirus, and Tulane virus, both in suspension and in different food matrices.<sup>23,30–32</sup> However, one of the major drawbacks to aqueous ozone is that it has a low dissolution rate and poor stability in water compared to other aqueous chemical inactivation agents.<sup>33</sup>

Microbubbles, with diameters ranging from 100 to 0.1  $\mu\text{m}$ , hold promise for enhancing the stability and dissolution rate of ozone in water.<sup>33,34,45</sup> Often, equipment and technology that generates microbubbles will also generate millimeter and nanometer (<0.1  $\mu\text{m}$ ) bubbles. Millimeter size bubbles often disappear shortly after aeration stops, whereas nanometer bubbles exist for a considerable amount of time.<sup>33,34,45</sup> Ozone microbubbles have also been reported to improve the inactivation efficacy of ozone against bacterial pathogens in complex environments. Phaephiphat et al. found that 7 min of contact between 1 ppm ozone microbubbles and *Salmonella* Typhimurium resulted in a 2.6  $\log_{10}$  reduction during vegetable washing.<sup>25</sup> Furthermore, there are complex pollutants in sewage including nonbiodegradable dyes or pesticide residue, and ozone microbubbles showed excellent removal rates during wastewater treatment.<sup>35,36</sup> Additional reports have demonstrated the antibacterial activity of ozone microbubbles on coliforms,<sup>37</sup> *Vibrio parahaemolyticus*,<sup>38</sup> and *Bacillus subtilis*.<sup>39</sup>

Although numerous studies exist suggesting the potential of microbubbles and ozone microbubbles against bacterial foodborne pathogens,<sup>25</sup> little work has been reported to investigate the efficacy of ozone microbubbles against noroviruses or their surrogates. The purpose of this study is to evaluate the potential of ozone microbubbles to serve as an aqueous inactivation agent in suspension over a short time period and compare its efficacy with that of aqueous ozone.

## 2. MATERIALS AND METHODS

**2.1. LLC-MK2 Preparation.** LLC-MK2 cells obtained from ATCC (ATCC CCL-7) were kept in liquid nitrogen, grown, and stored per the manufacturer instructions. Briefly, prior to each suspension assay, 1 mL of LLC-MK2 was thawed under room temperature, cultured in M199 growth media with 10% FBS (Gibco Fetal Bovine Serum, qualified, United States) and 1% pen-strep [Gibco Penicillin–Streptomycin (10,000 U/mL)], grown in T75 flasks, incubated at 37 °C 5% carbon dioxide for 4 days, and transferred to T150 flasks. To passage cells, 5 mL of 1X TrypLE (Gibco CTS TrypLE select enzyme) was added to each flask to break the connection between cells and the bottom of the flasks and then transferred to 15 mL of fresh M199 growth media (Gibco Medium 199, Earle's salts) as a neutralization buffer. The growth medium in each flask was renewed every 2 days. A T150 flask with LLC-MK2 has incubated for 4 days.<sup>40</sup> When a microscope was used to observe 95% confluent LLC-MK2 covering the bottom of the flask, the cells were ready for further experimental usage.

**2.2. Tulane Virus Preparation.** Tulane virus was provided by L.A. Jaykus (North Carolina State University). Viral stocks were inoculated in a T150 flask with 95% confluent LLC-MK2 and incubated in a 37 °C, 5% CO<sub>2</sub> incubator. After 4 days, the infected cells were frozen at −80 °C and thawed for three cycles and then harvested by centrifugation at 1810 rcf for 5 min. The supernatant was aliquoted into cryopreservation tubes (1 mL each) and kept at −80 °C again for further usage.<sup>40</sup> The final titer of Tulane virus was around 10<sup>7</sup> PFU/mL. Every sample used in this study was only freeze–thawed once.

**2.3. Suspension Assay.** Viral suspension assays were performed based on ASTM method E1052–11 with slight modification.<sup>41,42</sup> To measure the initial titer of LLC-MK2 cells, a 10 μL mixture of LLC-MK2 and 1X trypan blue was transferred to a cell counting slide and measured by a Bio-Rad Automated Cell Counter TC10. Then, the suspended LLC-MK2 cells were diluted in M199 growth media to 10 × 10<sup>6</sup> CFU/mL as the final concentration; then, the cells were seeded in 6-well plates and placed in a 37 °C, 5% CO<sub>2</sub> incubator overnight. To make an overlay solution, 2.4% Avicel solution (Sigma-Aldrich Avicel PH-101) was placed on a stir plate at least for 30 min and then mixed with 2X DMEM (Gibco DMEM, powder, high glucose, pyruvate) in equal parts to a final concentration of 1.2% Avicel. Tulane virus stock was taken from the −80 °C freezer and thawed at room temperature. A 1% sodium thiosulfate solution in water was prepared as a neutralization buffer.<sup>43</sup> Three control groups were used, including one neutralization control (1080 μL of 1% sodium thiosulfate solution premixed with 30 μL of disinfectant and 90 μL of Tulane virus), one cytotoxicity control [1080 μL of neutralization buffer, 90 μL of PBS (Corning Phosphate-Buffered Saline, 1X without calcium and magnesium, pH 7.4 ± 0.1), and 30 μL of disinfectant], and one nondisinfected control (1080 μL of neutralization buffer, 90 μL of Tulane virus, and 30 μL of PBS). After the injection of disinfectant into the virus, the mixture in a tube was placed on a tube revolver at a constant speed of 20 rpm/min for the desired time. Testing groups contained 120 μL mixtures of the Tulane virus sample and disinfectants and 1080 μL of neutralization buffer as a 1/10 dilution (Figure 1b).

**2.4. Plaque Assay.** Plaque assays were performed as previously reported.<sup>44</sup> −1 to −8 10-fold serial dilutions of neutralized virus and disinfectant in growth media were made, 400 μL of each dilution was added to the 6-well plates, and the plates were incubated in a 33 °C, 5% CO<sub>2</sub> incubator, gently tilted every 15 min. After an hour, 2 mL of the overlay solution was added to each well and put back in the same incubator for another 4 days. After 4 days of incubation, the Avicel agar was discarded, and then, 2 mL of formaldehyde (Fisher Science Education formaldehyde solution, 37%) that was 10-fold diluted in 1X DMEM media (Gibco DMEM, high glucose, no glutamine) was added. Formaldehyde was used to fix the cells and lock their cellular structure. After an hour of incubation at 33 °C, 5% CO<sub>2</sub>, all formaldehyde was disposed by washing with PBS, and crystal violet solution (Sigma-Aldrich crystal violet solution) was used to stain the cells. After 30 min of gentle shaking, PBS was used again to wash off the crystal violet stain.

### 2.5. Antiviral Agent Generation and Characterization.

The apparatus used for generating ozone microbubbles is shown in Figure 1a. An A2Z A2ZS-SGLAB (110 V) ozone generator generated 70 ppm ozone gas when the machine was

operating at maximum power (100%), produced around 0.18 mA of applied current, and filled with oxygen (Industrial grade Oxygen, Size 80 High-Pressure Steel Cylinder, CGA-540) at a 5 L/min input flow rate. The ozone output flow rate was controlled between 0 and 1 L/min, and the dissolved ozone concentration and water temperature were monitored by an ATi Q45H dissolved ozone transmitter. Microbubbles were injected into the water through a swirl flow-based nozzle (Eco-Bubble-S1, Taikohgiken Co, Japan) connected to a high-power Iwaki magnet pump MD-70RLZM-115 (water flow rate 14 L/min, ozone gas input flow rate 0.3 L/min, water temperature 21–26 °C). The bubble size distribution was monitored by the laser diffraction method (Mastersizer 3000, Malvern Instruments, United Kingdom), as exemplified in Figure 2. An ozone

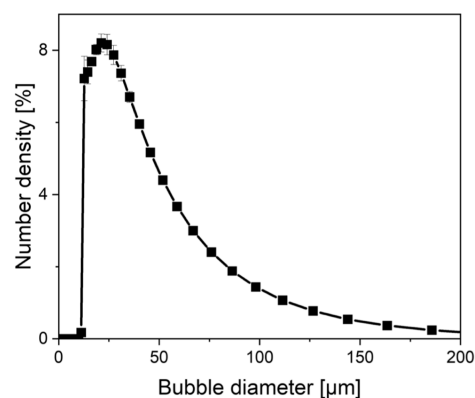


**Figure 2.** Size distribution of the ozone microbubbles used in this study. Bubble diameter was monitored by a laser diffraction method with 0.3 L/min of air flow rate and 14 L/min of water flow rate in 10 L of deionized water at 23 °C; mean diameters of bubbles were 36.15 ± 0.25 μm.

microbubble water solution was continuously circulated through the nozzle until the desired dissolved ozone concentration was attained. Nanobubbles (<0.1 μm) that were also produced by the nozzle were confirmed with a zetasizer (Malvern Instruments, United Kingdom) (data not shown). Aqueous ozone was acquired by continuously sparging ozone directly via an air stone (ozone gas input flow rate 1 L/min, water temperature 23 °C). Figure 3 illustrates an increasing trend in the dissolved ozone concentration. All experiments were conducted in a fume hood and repeated in triplicate on separate days.

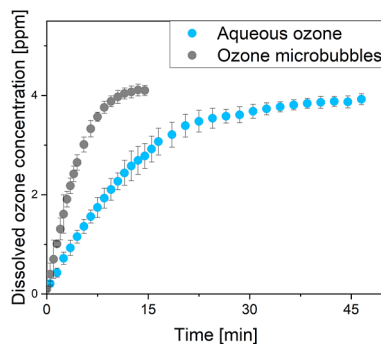


**Figure 3.** Ozone dissolution kinetics of ozone microbubbles by a microbubble generator (gray) and aqueous ozone by an air stone (blue).

**2.6. Effective Concentration of Dissolved Ozone for Virus Disinfection Treatment.** The ozone aeration process was halted upon reaching a dissolved ozone concentration of 4 ppm. Subsequently, the ozone microbubbles or aqueous ozone were allowed to remain within the water tank, undergoing natural degradation. As the ozone concentration gradually decreased, three specific time points (2, 10, and 20 min after the cessation of ozone aeration) were selected for the inactivation process before exposing the water to the virus. Figure 4 illustrates a declining trend in the dissolved ozone

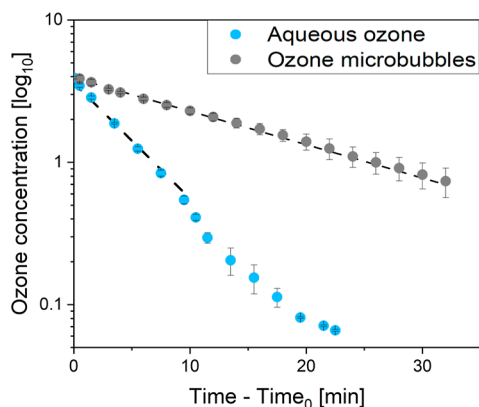


**Figure 4.** Degradation rate of ozone microbubbles (gray) and aqueous ozone (blue) in  $\log_{10}$  scale. The dissolved ozone concentration reached 4 ppm, which was time zero, and then, the ozone aeration was stopped. The dissolved ozone concentration degradation curve of ozone microbubbles and the first 10 min of aqueous ozone followed first-order kinetics.

concentration. For each time point, 120  $\mu\text{L}$   $10^7$  PFU/mL Tulane virus was treated with 40  $\mu\text{L}$  of generated ozone micro/bubbles. 120  $\mu\text{L}$  of the virus and the disinfectant mixture were then transferred to 1080  $\mu\text{L}$  of neutralization buffer (1% sodium thiosulfate in water) (sodium thiosulfate anhydrous (certified), Fisher Chemical)<sup>39</sup> to make a 1/10 dilution. After neutralization, the virus suspension was serially diluted in fresh M199 growth media, and each diluted sample was plated once to the 6-well plate during plaque assay. Untreated (PBS) and neutralization (preneutralized ozonated water and ozone microbubbles before the addition of virus) negative controls were used in each run. Suspension treatments were repeated in triplicate on separate days.

**2.7. Disinfection Durability Treatment.** The ozone concentration of aqueous ozone or ozone microbubbles was consistently maintained at 4 ppm equivalent point through continuous ozone gas aeration. 40  $\mu\text{L}$  of 4 ppm aqueous ozone or ozone microbubbles were transferred to 120  $\mu\text{L}$  of  $10^7$  PFU/mL virus suspension with gentle shaking for 15, 30, 60, and 120 s. Then, 120  $\mu\text{L}$  of treated virus solution was transferred to 1080  $\mu\text{L}$  of neutralization buffer to quench the residual ozone. The quantity of surviving virus was measured by a plaque assay. Suspension assays were repeated in triplicate on separate days.

**2.8. Organic Load Treatment.** The effectiveness of ozone microbubbles was tested in the presence of organic matter. The  $10^7$  PFU/mL virus sample was transferred to each FBS and M199 growth media mixture as a 1/10 dilution, and the final FBS concentrations in the samples were 0, 18, 36, 54, 72, and 90% FBS solutions (v/v). 40  $\mu\text{L}$  of 4 ppm ozone microbubbles was treated with 120  $\mu\text{L}$  of virus dilution with

gentle shaking on a tube revolver for 5 min. Then, the treated virus solution was diluted 1/10 with neutralization buffer. The quantity of surviving virus was measured by the plaque assay. Treatments were repeated in triplicate on separate days.

**2.9. Statistical Analysis.** All experimental results were repeated in triplicate and are shown as mean  $\pm$  standard deviation. Origin 2021b was used to calculate the statistical differences of all data by ANOVA (multiple comparisons) and *t*-test (pairwise comparisons), and  $p < 0.05$  was considered statistically significant.

### 3. RESULTS

**3.1. Kinetics of Ozone Dissolution and Degradation.** Figures 3 and 4 demonstrate the effect of microbubbles on the fast gas dissolution rate and extended stability. To achieve a concentration of 4 ppm, the ozone gas flow rate of ozone microbubbles generation was controlled at 0.3 L/min, while for the ozone sparging via the air stone, the ozone gas flow rate was 1 L/min, representing a more than 3-fold increase. In 10 L of deionized water, ozone microbubbles from the microbubble generator reached 4 ppm with a higher dissolution rate than the ozone sparging from the air stone (Figure 3). After the generation stopped, ozone microbubbles showed a longer half-life ( $14 \pm 0.81$  min) than the aqueous ozone ( $3 \pm 0.35$  min) (Figure 4). Similar to the previous study,<sup>41</sup> the ozone degradation curves followed first-order kinetics<sup>41</sup> at early times (dashed line, Figure 4). These results showed that ozone microbubbles had a significantly higher dissolution rate and a longer half-life than aqueous ozone.

**3.2. Ozone Durability of Antiviral Efficacy.** In order to investigate the relationship between inactivation efficacy and treatment time of aqueous ozone and ozone microbubbles,  $\log_{10}$  reduction values of Tulane virus are shown in Figure 5

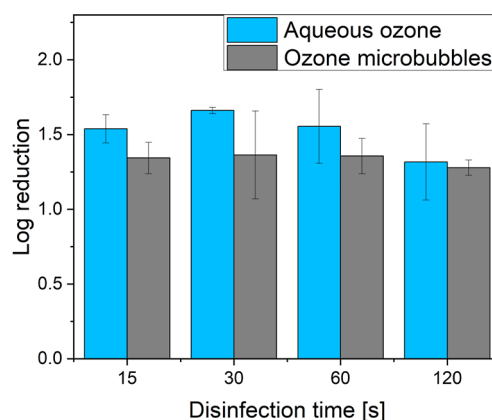


**Figure 5.** Inactivation ability of ozone microbubbles (gray) and aqueous ozone (blue) after 15, 30, 60, and 120 s of treatment time.

and Table 1. No significant differences were observed between aqueous ozone and ozone microbubbles groups or between each time point ( $p > 0.05$ ) (Figure 5 and Table 1). The residual ozone concentration for each time point was measured by a SenSafe Ozone Check Test Strip, and no ozone was left after 15 s of treatment. Virus inactivation occurs in a very short initial period and ozone was exhausted in the first 15 s, so little additional inactivation effect was observed during the remaining time; similar results were observed in the study of Lim et al.<sup>43</sup>

**Table 1. Inactivation Ability of Ozone Microbubbles and Aqueous Ozone after 15, 30, 60, and 120 s of Treatment Time**

disinfection time [s]	aqueous ozone [ $\log_{10}$ ]	ozone microbubbles [ $\log_{10}$ ]
15	1.54 ± 0.09	1.34 ± 0.1
30	1.66 ± 0.02	1.36 ± 0.29
60	1.55 ± 0.25	1.36 ± 0.12
120	1.32 ± 0.26	1.28 ± 0.05

**3.3. Effective Concentration of Dissolved Ozone for Virus Disinfection Treatment.** The efficacy of aqueous ozone and ozone microbubbles for Tulane virus disinfection was tested by evaluating their inactivation effectiveness at 2, 10, and 20 min after production, as depicted in Figure 6 and Table

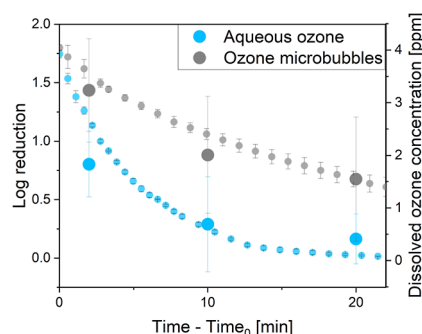


**Figure 6.** Inactivation ability of ozone microbubbles (gray) and aqueous ozone (blue) at 2, 10, and 20 min postgeneration, where the dissolved ozone concentration degradation is marked with dashed lines in the same color. The dissolved ozone concentration reached 4 ppm, which was time zero, and then the ozone aeration was stopped.

2 including residual ozone concentration. A significant difference between aqueous ozone versus ozone microbubbles was not observed using the experimental design tested here, where aqueous ozone or ozone microbubbles were pregenerated and then mixed with virus suspension. However, the inactivation efficacy of ozone reduced as ozone dissolved concentration decreased.<sup>33</sup> Microbubbles generated using air instead of ozone produced little to no inactivation (data not shown); therefore, ozone as an additional disinfectant is necessary for this study.

**3.4. Organic Load Disinfection Treatment.** To evaluate the ability of ozone microbubbles to inactivate Tulane virus in the presence of an organic load, inactivation experiments containing varying levels of FBS were conducted. After 5 min of contact with ozone microbubbles and Tulane virus, the reduction in viral titer was obtained and is shown in Figure 7 and Table 3. No significant difference was observed with the addition of FBS compared to the suspension of Tulane virus in buffer alone ( $p > 0.05$ ) (Figure 7).

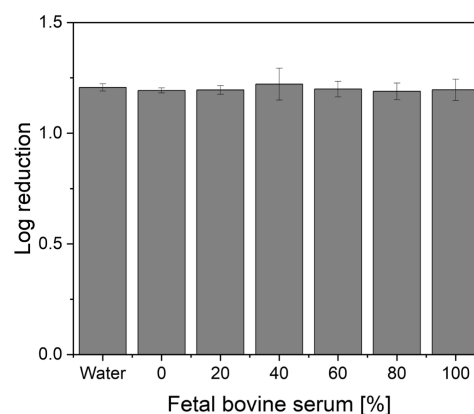


**Figure 7.** Influence of organic load on ozone microbubble inactivation of Tulane virus. Tulane virus was diluted 1/10 in a mixture of FBS and M199 growth media before ozone microbubble treatment.

**Table 3. Influence of Organic Load on Ozone Microbubble Inactivation of Tulane Virus**

solvent	ozone microbubbles [ $\log_{10}$ ]
water	1.21 ± 0.02
0% FBS	1.20 ± 0.01
18% FBS	1.20 ± 0.02
36% FBS	1.22 ± 0.07
54% FBS	1.20 ± 0.04
72% FBS	1.19 ± 0.04
90% FBS	1.20 ± 0.05

## 4. DISCUSSION

The degradation of aqueous ozone is rapid, but microbubbles can persist in water for a long period.<sup>46</sup> Because of their small size and high number, ozone microbubbles have been shown to promote the dissolution rate or stability of ozone, while also reducing the cost of inactivation treatment.<sup>47</sup> Another advantage of ozone microbubbles is their ability to be applied in larger aqueous settings in a potentially continuous manner. This work sought to investigate the efficacy of aqueous ozone and ozone microbubbles against the Tulane virus. Aqueous ozone requires higher gas input than ozone microbubbles to reach 4 ppm dissolved ozone concentration; thus, microbubbles require lower input gas for the equivalent amount of ozone. Based on the data presented here, it would also translate to comparable norovirus inactivation for less required input, thus providing cost savings and less required energy or environmental cost in ozone generation for antiviral applications.

Ozone, as a disinfectant, is often used in continuous virus inactivation experiments like vegetable washing or wastewater treatment,<sup>30,48</sup> but short contact time between ozone and virus also displayed inactivation efficacy. The inactivation of ozone on the Tulane virus has previously been reported to be

**Table 2. Inactivation Ability and Residual Concentration of Ozone Microbubbles and Aqueous Ozone at 2, 10, and 20 min Postgeneration**

ozone postgenerated time [min]	aqueous ozone concentration [ppm]	aqueous ozone [ $\log_{10}$ ]	ozone microbubbles concentration [ppm]	ozone microbubbles [ $\log_{10}$ ]
2	2.52 ± 0.07	0.8 ± 0.28	3.2 ± 0.2	1.43 ± 0.44
10	0.43 ± 0.05	0.29 ± 0.41	2.26 ± 0.19	0.88 ± 0.5
20	0.09 ± 0.01	0.16 ± 0.21	1.49 ± 0.23	0.68 ± 0.53

proportional to the dissolved ozone concentration applied. In a noncontinuous treatment, Thurston-Enriquez et al. observed 4.28 and 1.85  $\log_{10}$  reduction of feline calicivirus in suspension in 0.25 min of 1 and 0.06 ppm aqueous ozone exposure, respectively. Ozone degradation happened rapidly during the inactivation treatment.<sup>49</sup> Similarly, little dissolved ozone was left after 15 s of treatment in this study, which may explain why the duration of virus exposure to ozone did not affect the inactivation efficacy during the noncontinuous treatment reported here. In fact, some time points with longer treatment displayed slightly lower inactivation than that with less treatment, and this is due to the inherent variability of suspension and plaques assays, which is further evidenced by the fact that there was no statistical significance between any of the treatment time points (Figure 5). The time points tested here were shorter than those tested in continuous applications, and it is likely that all of the ozone reacted rather quickly, which also may explain why additional inactivation did not occur at extended time points. Overall, the levels of reduction observed here would not be considered very efficacious for a chemical surface disinfectant application against noroviruses as the methodology used here is similar to what would be performed in a traditional suspension assay for evaluating such disinfectants. However, it is quite possible that if aqueous ozone or ozone microbubbles were continuously generated throughout the reported incubation times with the virus, more inactivation would be observed than what has been reported with aqueous ozone. The work by Choi et al. suggested that Tulane virus was continuously exposed to 1 ppm aqueous ozone and a 4.18  $\log_{10}$  virus titer reduction was observed in 4 min.<sup>50</sup> This should be investigated in future study as such treatment could be feasible in a produce wash tank or water treatment applications.

In this study, microbubbles extended the ozone half-life from 3 to 14 min, but only the first 10 min after production can ensure its inactivation efficacy in Tulane virus suspension ( $>1 \log_{10}$ ). Although the observed inactivation was not considered to be an ideal level for a surface disinfectant, the possibility that continuous generation of ozone microbubbles could enhance inactivation in aqueous food processing settings (production of wash tanks, water treatment, etc.) and the use of microbubbles could extend the ozone half-life and potentially improve inactivation efficacy in larger scale aqueous settings. However, future work is needed to investigate this. Interestingly, microbubbles generated in the ambient atmosphere did not result in any observable inactivation of the Tulane virus in our preliminary work (data not shown). Nghia et al. demonstrated that using air, oxygen, and ozone nanobubbles with oxidation–reduction potentials of 315 mV, 355 mV, and 830 mV against *V. parahemolyticus* in 1.5% saline water, air and oxygen nanobubbles produced 0.16 and 0.33  $\log_{10}$  reductions against *V. parahemolyticus*, respectively, with treatment occurring for 60 min once a day for 7 days, and the ozone nanobubble was applied for 6 min a day for 7 days and resulted in a 2  $\log_{10}$  reduction.<sup>38</sup> This suggests that the inactivation observed in this report from ozone microbubbles was likely mostly due to the presence of the ozone. This also may explain why similar levels of inactivation between aqueous ozone and ozone microbubbles were observed.

FBS is a common cell culture supplement, composed of a mixture of macromolecules, including enzymes, amino acids, carbohydrates, vitamins, and minerals that have been traditionally used as a synthetic proxy to introduce organic load in

the study of viral inactivation.<sup>51–53</sup> The presence of FBS or cell growth media (organic load) typically has been shown to reduce the efficacy of numerous different chemical inactivation agents against viruses compared to that of the treatment with the agent in buffer alone.<sup>52</sup> The evaluation of these agents in the presence of organic load is especially relevant as this reflects potential real-world applications for action against the virus in food products or unclean environmental surfaces. The results from this report suggest that even in the presence of relatively high levels of FBS media, ozone microbubbles demonstrated viral inactivation similar to that of buffer alone (Figure 7). This would suggest that this treatment may show promise in food production applications, which should be the subject of future research. However, it is possible that in the continuous application of aqueous ozone or ozone microbubbles over longer treatment times, the effect of FBS could become pronounced, and this would also be an important subject for future study. Another potential explanation for the lack of effect of FBS could be due to the fact that suspension treatment was performed with constant agitation using a tube flipper, as a similar observation was reported by Wenzel et al.<sup>54</sup> Specifically, rat fibroblast damage during 8.17 ppm ozone exposure was found to depend on the incubation of the cells with FBS without agitation, but in the rotated exposure model, FBS did not have a significant effect. Wenzel et al. suggest that the free radicals and peroxides produced by ozone were the reasons for cells damage, so in the stationary model, FBS had a long time to react with these byproducts and reduce the ozone inactivation efficacy, while ozone could more readily directly contact cells in the rotated model rather than being quenched by FBS.<sup>54</sup> In the work reported here, a similar gentle agitation using rotation was applied, and this could potentially have resulted in a similar effect. In the study of fluorescent lamp damage to human D98/AH2 cells, Wang et al. found that more hydrogen peroxide was generated in the presence of riboflavin and tryptophan.<sup>55</sup> These components are also present in the M199 growth media we used in this work with FBS for organic load simulation. Additionally, Takeda et al. reported that 500 ppm ozonated glycerol treatment of SARS-CoV-2 resulted in higher inactivation in the presence of 20 and 40% FBS than with 1% FBS.<sup>56</sup> It was suggested that the residual ozone concentration still can have sufficient oxidizing ability after a reaction with FBS, especially in the presence of added iron ions during treatment to maintain or enhance inactivation efficacy.<sup>56</sup> These effects may also explain why no protective effect of the FBS medium on viral inactivation was observed here. However, this would make the subject of an interesting future work that could inform the potential application of this system to different foods.

Many inactivation agents have been shown to display limited efficacy against Tulane virus, especially those approved for application on foods and food surfaces.<sup>23,57–59</sup> Wang et al. evaluated the efficacy of aqueous ozone on alfalfa seeds. 6.25 ppm aqueous ozone was constantly introduced to the water with Tulane virus-inoculated alfalfa seeds and  $1.66 \pm 1.11$  to  $3.83 \pm 1.01 \log_{10}$  reduction values of Tulane virus observed after 0.5 to 30 min of treatment, respectively.<sup>32</sup> A similar experimental model was mentioned in the study of Lim et al., where 2 min of 1 ppm aqueous ozone exposure produced more than 2  $\log_{10}$  reduction of murine norovirus in suspension.<sup>43</sup> The higher level of inactivation efficacy was attributed to the larger disinfectant usage dose. To the author's knowledge, no

quantitative data on ozone microbubbles or microbubble treatment of a norovirus surrogate have been reported to date.

## 5. CONCLUSIONS

This article demonstrates that aqueous ozone and ozone microbubbles produced more than 1 log<sub>10</sub> reduction against Tulane virus over a relatively short duration of exposure, including in the presence of a relatively high organic load (FBS media). After noncontinuous treatment of pregenerated disinfectants, aqueous ozone produced an inactivation effect only in the first 2 min and ozone microbubbles maintained the inactivation efficacy for 10 min. These results suggest that future work investigating a continuous production of aqueous ozone or ozone microbubbles over longer periods in aqueous applications relevant to foods implicated in norovirus transmission could be of value. This study suggests that future work evaluating the antiviral efficacy of ozone microbubbles against nonenveloped viruses in various matrices, which has been hitherto underexplored, is warranted.

## ■ ASSOCIATED CONTENT

### Data Availability Statement

The data presented in this study are provided in the Supporting Information.

### SI Supporting Information

The Supporting Information is available free of charge at <https://pubs.acs.org/doi/10.1021/acsomega.3c08396>.

Data for ozone dissolution, ozone degradation, bubble distribution, disinfection durability, effective concentration of dissolved ozone, organic load, air microbubbles, and residual ozone (XLSX)

## ■ AUTHOR INFORMATION

### Corresponding Authors

**Jiakai Lu** – Department of Food Science, University of Massachusetts, Amherst, Massachusetts 01003, United States; Phone: 413-577-7194; Email: [jiakailu@umass.edu](mailto:jiakailu@umass.edu)

**Matthew D. Moore** – Department of Food Science, University of Massachusetts, Amherst, Massachusetts 01003, United States; [orcid.org/0000-0002-5393-0733](https://orcid.org/0000-0002-5393-0733); Phone: 1-413-545-1019; Email: [mdmoore@umass.edu](mailto:mdmoore@umass.edu)

### Authors

**Bozhong Guan** – Department of Food Science, University of Massachusetts, Amherst, Massachusetts 01003, United States

**Haknyeong Hong** – Department of Food Science, University of Massachusetts, Amherst, Massachusetts 01003, United States

**Minji Kim** – Department of Food Science, University of Massachusetts, Amherst, Massachusetts 01003, United States; [orcid.org/0000-0002-8926-9449](https://orcid.org/0000-0002-8926-9449)

Complete contact information is available at:

<https://pubs.acs.org/10.1021/acsomega.3c08396>

### Author Contributions

Conceptualization: M.D.M., J.L., B.G., and H.H.; methodology: M.D.M., J.L., B.G., and H.H.; software: B.G.; validation: B.G. and H.H.; formal analysis: B.G. and H.H.; investigation: M.D.M., J.L., B.G., and H.H.; resources: M.D.M. and J.L.; data curation: M.D.M., J.L., B.G., and H.H.; writing—original draft preparation: B.G. and H.H.; writing—review and editing: M.D.M., J.L., B.G., M.K., and H.H.; visualization: M.K., B.G.,

and H.H.; supervision: M.D.M. and J.L.; project administration: M.D.M. and J.L.; and funding acquisition: M.D.M. and J.L. All authors have read and agreed to the published version of the manuscript.

### Funding

This research and the APC were funded by the University of Massachusetts, Amherst.

### Notes

The authors declare no competing financial interest.

## ■ REFERENCES

- (1) Kirk, M. D.; Pires, S. M.; Black, R. E.; Caipo, M.; Crump, J. A.; Devleeschauwer, B.; Döpfer, D.; Fazil, A.; Fischer-Walker, C. L.; Hald, T.; Hall, A. J.; Keddy, K. H.; Lake, R. J.; Lanata, C. F.; Torgerson, P. R.; Havelaar, A. H.; Angulo, F. J. Correction: World Health Organization estimates of the global and regional disease burden of 22 foodborne bacterial, protozoal, and viral diseases, 2010: a data synthesis. *PLoS Med.* **2015**, *12* (12), No. e1001940.
- (2) Scallan, E.; Hoekstra, R. M.; Angulo, F. J.; Tauxe, R. V.; Widdowson, M. A.; Roy, S. L.; Jones, J. L.; Griffin, P. M. Food-borne illness acquired in the United States—major pathogens. *Emerging Infect. Dis.* **2011**, *17* (1), 7–15.
- (3) Teunis, P. F.; Moe, C. L.; Liu, P. E.; E Miller, S.; Lindesmith, L.; Baric, R. S.; Le Pendu, J.; Calderon, R. L. Norwalk virus: how infectious is it? *J. Med. Virol.* **2008**, *80* (8), 1468–1476.
- (4) Sabrià, A.; Pintó, R. M.; Bosch, A.; Bartolomé, R.; Cornejo, T.; Torner, N.; Martínez, A.; Simón, M. d.; Domínguez, A.; Guix, S. Norovirus shedding among food and healthcare workers exposed to the virus in outbreak settings. *J. Clin. Virol.* **2016**, *82*, 119–125.
- (5) McMenemy, P.; Kleczkowski, A.; Lees, D. N.; Lowther, J.; Taylor, N. A model for estimating pathogen variability in shellfish and predicting minimum depuration times. *PLoS One* **2018**, *13* (3), No. e0193865.
- (6) Seitz, S. R.; Leon, J. S.; Schwab, K. J.; Lyon, G. M.; Dowd, M.; McDaniels, M.; Abdulhafid, G.; Fernandez, M. L.; Lindesmith, L. C.; Baric, R. S.; Moe, C. L. Norovirus infectivity in humans and persistence in water. *Appl. Environ. Microbiol.* **2011**, *77* (19), 6884–6888.
- (7) Tung, G.; Macinga, D.; Arbogast, J.; Jaykus, L. A. Efficacy of commonly used disinfectants for inactivation of human noroviruses and their surrogates. *J. Food Prot.* **2013**, *76* (7), 1210–1217.
- (8) Tian, P.; Yang, D.; Quigley, C.; Chou, M.; Jiang, X. Inactivation of the Tulane virus, a novel surrogate for the human norovirus. *J. Food Prot.* **2013**, *76* (4), 712–718.
- (9) Jeong, M. I.; Park, S. Y.; Ha, S. D. Effects of sodium hypochlorite and peroxyacetic acid on the inactivation of murine norovirus-1 in Chinese cabbage and green onion. *LWT* **2018**, *96*, 663–670.
- (10) Ha, J. H.; Choi, C.; Lee, H. J.; Ju, I. S.; Lee, J. S.; Ha, S. D. Efficacy of chemical disinfectant compounds against human norovirus. *Food Control* **2016**, *59*, 524–529.
- (11) Tudela, J. A.; López-Gálvez, F.; Allende, A.; Hernández, N.; Andújar, S.; Marín, A.; Garrido, Y.; Gil, M. I. Operational limits of sodium hypochlorite for different fresh produce wash water based on microbial inactivation and disinfection by-products (DBPs). *Food Control* **2019**, *104*, 300–307.
- (12) Boorman, G. A. Drinking water disinfection byproducts: review and approach to toxicity evaluation. *Environ. Health Perspect.* **1999**, *107* (suppl 1), 207–217.
- (13) Nieuwenhuijsen, M. J.; Toledano, M. B.; Eaton, N. E.; Fawell, J.; Elliott, P. Chlorination disinfection byproducts in water and their association with adverse reproductive outcomes: a review. *Occup. Environ. Med.* **2000**, *57* (2), 73–85.
- (14) Lin, Q.; Lim, J. Y.; Xue, K.; Yew, P. Y. M.; Owh, C.; Chee, P. L.; Loh, X. J. Sanitizing agents for virus inactivation and disinfection. *View* **2020**, *1* (2), No. e16.

- (15) Bintsis, T.; Litopoulou-Tzanetaki, E.; Robinson, R. K. Existing and potential applications of ultraviolet light in the food industry - a critical review. *J. Food Sci. Agric.* **2000**, *80*, 637–645.
- (16) DeSesso, J. M.; Harris, S. B.; Scialli, A. R.; Williams, A. L. Systematic assessment of quaternary ammonium compounds for the potential to elicit developmental and reproductive effects. *Birth Defects Res.* **2021**, *113* (20), 1484–1511.
- (17) Gilling, D. H.; Kitajima, M.; Torrey, J. R.; Bright, K. R. Antiviral efficacy and mechanisms of action of oregano essential oil and its primary component carvacrol against murine norovirus. *J. Appl. Microbiol.* **2014**, *116* (5), 1149–1163.
- (18) Moore, M. D.; Goulter, R. M.; Jaykus, L. A. Human norovirus as a foodborne pathogen: challenges and developments. *Annu. Rev. Food Sci. Technol.* **2015**, *6*, 411–433.
- (19) Li, X.; Huang, R.; Chen, H. Evaluation of assays to quantify infectious human norovirus for heat and high-pressure inactivation studies using Tulane virus. *Food Environ. Virol.* **2017**, *9*, 314–325.
- (20) Kniel, K. E. The makings of a good human norovirus surrogate. *Curr. Opin. Virol.* **2014**, *4*, 85–90.
- (21) Yu, G.; Zhang, D.; Guo, F.; Tan, M.; Jiang, X.; Jiang, W. Cryo-EM structure of a novel calicivirus, Tulane virus. *PLoS One* **2013**, *8* (3), No. e59817.
- (22) Farkas, T.; Cross, R. W.; Hargitt, E., III; Lerche, N. W.; Morrow, A. L.; Sestak, K. Genetic diversity and histo-blood group antigen interactions of rhesus enteric caliciviruses. *J. Virol.* **2010**, *84* (17), 8617–8625.
- (23) Predmore, A.; Sanglay, G.; Li, J.; Lee, K. Control of human norovirus surrogates in fresh foods by gaseous ozone and a proposed mechanism of inactivation. *Food Microbiol.* **2015**, *50*, 118–125.
- (24) Polo, D.; Álvarez, C.; Díez, J.; Darriba, S.; Longa, A.; Romalde, J. L. Viral elimination during commercial depuration of shellfish. *Food Control* **2014**, *43*, 206–212.
- (25) Phaephiphat, A.; Mahakarnchanakul, W. Surface decontamination of Salmonella Typhimurium and Escherichia coli on sweet basil by ozone microbubbles. *Cogent Food Agric.* **2018**, *4* (1), 1558496.
- (26) Chuajedton, A.; Uthaiutra, J.; Whangchai, K.; Nuanaon, N. Ozone microbubbles disinfection technique to inactivate penicillium digitatum in suspension. *Acta Hort.* **2015**, *1088*, 355–358.
- (27) He, H.; Zheng, L.; Li, Y.; Song, W. Research on the feasibility of spraying micro/nano bubble ozonated water for airborne disease prevention. *Ozone: Sci. Eng.* **2015**, *37* (1), 78–84.
- (28) Robert Jay, R.; Howard, R. A plausible “penny” costing effective treatment for corona virus-ozone therapy. *J. Infect Dis Epidemiol* **2020**, *6* (2), 113.
- (29) Tizaoui, C. Ozone: a potential oxidant for COVID-19 virus (SARS-CoV-2). *Ozone: Sci. Eng.* **2020**, *42* (5), 378–385.
- (30) Hirneisen, K. A.; Markland, S. M.; Kniel, K. E. Ozone inactivation of norovirus surrogates on fresh produce. *J. Food Prot.* **2011**, *74* (5), 836–839.
- (31) Brié, A.; Boudaud, N.; Mssihid, A.; Loutreul, J.; Bertrand, I.; Gantzer, C. Inactivation of murine norovirus and hepatitis A virus on fresh raspberries by gaseous ozone treatment. *Food Microbiol.* **2018**, *70*, 1–6.
- (32) Wang, Q.; Markland, S.; Kniel, K. E. Inactivation of human norovirus and its surrogates on alfalfa seeds by aqueous ozone. *J. Food Prot.* **2015**, *78* (8), 1586–1591.
- (33) Kobayashi, F.; Ikeura, H.; Ohsato, S.; Goto, T.; Tamaki, M. Disinfection using ozone microbubbles to inactivate Fusarium oxysporum f. sp. melonis and Pectobacterium carotovorum subsp. carotovorum. *Crop Prot.* **2011**, *30* (11), 1514–1518.
- (34) Lu, J.; Jones, O. G.; Yan, W.; Corvalan, C. M. Microbubbles in Food Technology. *Annu. Rev. Food Sci. Technol.* **2023**, *14*, 495–515.
- (35) Chu, L. B.; Xing, X. H.; Yu, A. F.; Zhou, Y. N.; Sun, X. L.; Jurcik, B. Enhanced ozonation of simulated dyestuff wastewater by microbubbles. *Chemosphere* **2007**, *68* (10), 1854–1860.
- (36) Ikeura, H.; Takahashi, H.; Kobayashi, F.; Sato, M.; Tamaki, M. Effects of microbubble generation methods and dissolved oxygen concentrations on growth of Japanese mustard spinach in hydroponic culture. *J. Hortic. Sci. Biotechnol.* **2018**, *93* (5), 483–490.
- (37) Sumikura, M.; Hidaka, M.; Murakami, H.; Nobutomo, Y.; Murakami, T. Ozone microbubble disinfection method for wastewater reuse system. *Water Sci. Technol.* **2007**, *56* (5), 53–61.
- (38) Nghia, N. H.; Van, P. T.; Giang, P. T.; Hanh, N. T.; St-Hilaire, S.; Domingos, J. A. Control of Vibrio parahaemolyticus (AHPND strain) and improvement of water quality using nanobubble technology. *Aquacult. Res.* **2021**, *52* (6), 2727–2739.
- (39) Tsuge, H.; Li, P.; Shimatani, N.; Shimamura, Y.; Nakata, H.; Ohira, M. Fundamental study on disinfection effect of microbubbles. *Kagaku Kogaku Ronbunshu* **2009**, *35* (5), 548–552.
- (40) Farkas, T.; Sestak, K.; Wei, C.; Jiang, X. Characterization of a rhesus monkey calicivirus representing a new genus of Caliciviridae. *J. Virol.* **2008**, *82* (11), 5408–5416.
- (41) Moorman, E.; Montazeri, N.; Jaykus, L. A. Efficacy of neutral electrolyzed water for inactivation of human norovirus. *Appl. Environ. Microbiol.* **2017**, *83* (16), No. e00653–17.
- (42) ASTM International. *E1052–11 Standard test method to assess the activity of microbicides against viruses in suspension*; ASTM, 2011.
- (43) Lim, M. Y.; Kim, J. M.; Lee, J. E.; Ko, G. Characterization of ozone disinfection of murine norovirus. *Appl. Environ. Microbiol.* **2010**, *76* (4), 1120–1124.
- (44) Vaze, N.; Soorneedi, A. R.; Moore, M. D.; Demokritou, P. Inactivating SARS-CoV-2 Surrogates on Surfaces Using Engineered Water Nanostructures Incorporated with Nature Derived Antimicrobials. *Nanomaterials* **2022**, *12* (10), 1735.
- (45) Batagoda, J. H.; Hewage, S. D. A.; Meegoda, J. N. Nano-ozone bubbles for drinking water treatment. *J. Environ. Eng. Sci.* **2019**, *14* (2), 57–66.
- (46) Meegoda, J. N.; Aluthgun Hewage, S.; Batagoda, J. H. Stability of nanobubbles. *Environ. Eng. Sci.* **2018**, *35* (11), 1216–1227.
- (47) Jyoti, K. K.; Pandit, A. B. Ozone and cavitation for water disinfection. *Biochem. Eng. J.* **2004**, *18* (1), 9–19.
- (48) Gomes, J.; Frasson, D.; Quinta-Ferreira, R. M.; Matos, A.; Martins, R. C. Removal of enteric pathogens from real wastewater using single and catalytic ozonation. *Water* **2019**, *11* (1), 127.
- (49) Thurston-Enriquez, J. A.; Haas, C. N.; Jacangelo, J.; Gerba, C. P. Inactivation of enteric adenovirus and feline calicivirus by ozone. *Water Res.* **2005**, *39* (15), 3650–3656.
- (50) Choi, J. M.; D’Souza, D. H. Inactivation of Tulane virus and feline calicivirus by aqueous ozone. *J. Food Sci.* **2023**, *88* (10), 4218–4229.
- (51) Subbiahannadar Chelladurai, K.; Selvan Christyraj, J. D.; Rajagopalan, K.; Yesudhasan, B. V.; Venkatchalam, S.; Mohan, M.; Chellathurai Vasantha, N.; Selvan Christyraj, J. R. S. Alternative to FBS in animal cell culture-An overview and future perspective. *Heliyon* **2021**, *7* (8), No. e07686.
- (52) Kamarasu, P.; Hsu, H. Y.; Moore, M. D. Research progress in viral inactivation utilizing human norovirus surrogates. *Front. Sustain. Food Syst.* **2018**, *2*, 89.
- (53) Sangsratanakul, N.; Toyofuku, C.; Suzuki, M.; Komura, M.; Yamada, M.; Alam, M. S.; Ruenphet, S.; Shoham, D.; Sakai, K.; Takehara, K. Virucidal efficacy of food additive grade calcium hydroxide against surrogate of human norovirus. *J. Virol. Methods* **2018**, *251*, 83–87.
- (54) Wenzel, D. G.; Morgan, D. L. Role of in vitro factors in ozone toxicity for cultured rat lung fibroblasts. *Drug Chem. Toxicol.* **1982**, *5* (3), 201–217.
- (55) Wang, R. J.; Nixon, B. T. Identification of hydrogen peroxide as a photoproduct toxic to human cells in tissue-culture medium irradiated with “daylight” fluorescent light. *In Vitro* **1978**, *14* (8), 715–722.
- (56) Takeda, Y.; Jamsransuren, D.; Makita, Y.; Kaneko, A.; Matsuda, S.; Ogawa, H.; Oh, H. Inactivation of SARS-CoV-2 by Ozonated Glycerol. *Food Environ. Virol.* **2021**, *13* (3), 316–321.
- (57) Hirneisen, K. A.; Kniel, K. E. Comparing human norovirus surrogates: murine norovirus and Tulane virus. *J. Food Prot.* **2013**, *76* (1), 139–143.

(58) Arthur, S. E.; Gibson, K. E. Physicochemical stability profile of Tulane virus: a human norovirus surrogate. *J. Appl. Microbiol.* **2015**, *119* (3), 868–875.

(59) Cromeans, T.; Park, G. W.; Costantini, V.; Lee, D.; Wang, Q.; Farkas, T.; Lee, A.; Vinjé, J. Comprehensive comparison of cultivable norovirus surrogates in response to different inactivation and disinfection treatments. *Appl. Environ. Microbiol.* **2014**, *80* (18), 5743–5751.